



ELSEVIER

Surface Science 375 (1997) L379–L384

surface science

## Surface Science Letters

# Threshold resonances in classical chaotic atom–surface scattering

R. Guantes <sup>a</sup>, F. Borondo <sup>a</sup>, J. Margalef-Roig <sup>b</sup>, S. Miret-Artés <sup>c,\*</sup>, J.R. Manson <sup>c,1</sup>

<sup>a</sup> Departamento de Química, C-IX, Universidad Autónoma de Madrid, Cantoblanco-28049 Madrid, Spain

<sup>b</sup> Instituto de Matemáticas y Física Fundamental, Consejo Superior de Investigaciones Científicas, Serrano 123, 28006 Madrid, Spain

<sup>c</sup> Max-Planck-Institut für Strömungsforschung, Bunsenstrasse 10, D-37073 Göttingen, Germany

Received 4 October 1996; accepted for publication 20 December 1996

### Abstract

A classical picture of threshold resonances in diffractive systems is provided in the light of a new classical singularity recently predicted for atom surface scattering, the skipping singularity. As an illustration of these dynamics, application to the scattering of He atoms by the stepped Cu(115) surface is presented using both a hard corrugated one-dimensional wall and a corrugated Morse potential. It is also emphasized that these resonances are observable for highly corrugated surfaces or for surfaces with weak corrugation but at incident conditions where multiple scattering is important. © 1997 Elsevier Science B.V. All rights reserved.

**Keywords:** Atom–solid interactions, scattering, diffraction; Atom–solid scattering and diffraction – elastic; Copper; Vicinal single crystal surfaces

Threshold resonances (TR) or emerging beam resonances are a very general feature of diffractive systems and should be observed whenever the initial conditions of incidence for the scattering particle are such that a new diffraction beam just becomes visible [1]. Due to the sum rule (unitary condition), this *resonance* behavior is manifest in the intensity of all diffracted peaks although the effect may be very weak. However it is expected to be experimentally detectable for highly corrugated surfaces [2] and has been observed for rotational diffraction [3]. As a result, the appearance or disappearance of a beam is always accompanied by a divergence in the slope of any diffracted beam

with respect to one of the initial values ( $k_i, \theta_i, \phi_i$ ) determining the scattering geometry. Often in the experimental configurations the diffracted intensities are measured as a function of the incident polar angle with the incident energy and azimuthal angle held constant. Moreover, the angle between the source and the detector ( $\theta_{SD} = \theta_i + \theta_f$ ) is often fixed at  $\pi/2$  or greater. In atomic and molecular surface scattering, TR are expected to provide additional information about the long range part of the interaction potential.

In a recent paper [4], we have reported a new type of classical singularity occurring only for diffractive systems and when the deflection or final angle of the particles is equal to  $\pm\pi/2$ . It is called the *skipping singularity* since a classical image of this singular behavior can be given by the skipping of stones on the surface of a river. In order to skip

\* Corresponding author. Fax: +34 1 5854894;  
e-mail: salvador@cc.csic.es

<sup>1</sup> Permanent address: Department of Physics and Astronomy, Clemson University, Clemson, SC 29634, USA.

a stone on a river it is necessary not only to get the correct incident angle but also to strike specific impact points on ripples of the water surface. At the same time, the onset of classical trapping, that is classical chaos, takes place when a surface rainbow angle simultaneously reaches  $\pm\pi/2$  [5–7]. This condition implies that the scattering particle is travelling parallel to the surface and will probably encounter the surface more than once. Within the framework of the hard wall approximation, for any incident energy the surface rainbow angles are dependent on the incident scattering angle, and occur at certain impact parameters  $b$  (or impact points on the surface) which correspond to the inflection points of the surface. However, above a given threshold value of the incident angle, not only do the inflection points of the surface lead to this classical trapping but also additional impact parameters contribute to this trapping. If plots of  $\theta_i$  versus  $b$  are analyzed, the region of these impact parameters is delimited by the two branches of a concave curve in such a way that the area inside this curve corresponds to multiple scattering events and the outer area to single scattering events. In other words, the rainbow singularity *bifurcates* into the two branches of a curve which define the skipping singularity (bifurcation diagram) and its minimum gives the threshold value of the incident angle for chaos. This temporary (vibrational) trapping has been conjectured to be associated with selective adsorption resonances leading to a classical picture of such resonances. Obviously, not all trapped or chaotic trajectories contribute to a given resonance process but this discussion will be postponed for a future work [8]. In a certain sense this singularity could be the counterpart of the very well known *orbiting singularity* in the scattering of two particles by a central field. This singularity corresponds physically to the mutual capture of the colliding particles for a finite time after forming a rotating system.

In this Letter, our main goal is to relate TR with the skipping and rainbow singularities. Although the denomination TR is somewhat misleading, since we are not dealing with true resonances or quasi-bound states, as we will show later, this standard terminology coming from

diffraction physics becomes more apparent in a classical framework. For this purpose, two functions are introduced. The first one is the classical deflection (CD) function which is defined as the variation of the final or outgoing angle of the scattering particles as a function of  $b$ . The second one, originally introduced by Masel et al. [9] in this context, is called the diffraction order (DO) function which gives the parallel momentum transfer in the scattering process also as a function of  $b$ . When the skipping singularity takes place, the DO function also bifurcates as we have recently shown [4].

For any elastic scattering process, the conservation rules of energy and parallel momentum result in the following expression:

$$k_{Gz}^2 = k_i^2 - (\mathbf{K} + \mathbf{G})^2, \quad (1)$$

where the incident particle wave vector is  $\mathbf{k}_i = (\mathbf{K}_i, k_{iz})$  and the final one is written as  $\mathbf{k}_G = (\mathbf{K}_i + \mathbf{G}, k_{Gz})$ ,  $\mathbf{G}$  being a reciprocal lattice vector. Here by  $N$  will be denoted the reciprocal lattice vector associated with an emerging beam ( $k_{Nz}^2 \rightarrow 0$ ).

Now let us consider the classical in-plane diffracted intensity as formulated in Ref. [9] for a one-dimensional corrugation surface to be

$$I_J(k_i, \theta_i) = \sum_j \left| \frac{dJ(b_j; k_i, \theta_i)}{db} \right|^{-1}, \quad (2)$$

where  $\theta_i$  is the incident scattering angle and  $b$  the normalized impact parameter defined by  $b = x/a$  along the  $x$  direction with  $a$  being the surface unit cell length in that direction. The sum is over all values of the impact parameter  $b_j$  that contribute to a given integer value,  $J$ , of the DO function  $J(b; k_i, \theta_i)$ . This function arises as an alternative way to express the diffraction condition as

$$J(b; k_i, \theta_i) = \frac{a}{2\pi} k_i [\sin \theta_f(b) - \sin \theta_i], \quad (3)$$

where  $\theta_f(b)$  is the well-known CD function defined [4] by

$$\theta_f(b) = \theta_i \pm 2 \left| \tan^{-1} \frac{\xi'(b)}{a} \right|, \quad (4)$$

where the  $+$  sign is used when the  $\tan^{-1}$  function

gives negative angles and the  $-$  sign otherwise;  $\xi(x)$  is the corrugation or shape function and  $\xi'(x)$  its first derivative with respect to  $b$ . For simplicity in the exposition we prefer to use a 1D formulation here, but this theory can be readily extended to 2D corrugated surfaces.

Classically, Eq. (2) gives the envelope of the diffraction pattern. In order to obtain the intensity in each of the diffraction channels or Bragg directions one evaluates this function for integer values of the diffraction order,  $J$ . The classical diffracted intensity will present singularities whenever the derivative of the DO function with respect to the impact parameter is zero:

$$\left( \frac{dJ(b; k_i, \theta_i)}{db} \right)_{b=b_j} = 0. \quad (5)$$

Using the chain rule and assuming an experiment done at constant energy, this condition can be rewritten as:

$$\left( \frac{dJ(\theta_f; k_i, \theta_i)}{d\theta_f} \right) \left( \frac{d\theta_f(b)}{db} \right)_{b=b_j} = 0. \quad (6)$$

Clearly if either of these two factors (or both) is equal to zero they give rise to singularities in the scattering intensity. Zero values of the first factor give rise to the classical skipping singularity [4] and zero values of the second factor correspond to the well-known surface rainbows. Now the zero values of the first factor can be obtained by differentiating Eq. (3), yielding

$$\left( \frac{dJ(\theta_f; k_i, \theta_i)}{d\theta_f} \right) = \frac{a}{2\pi} k_i \cos \theta_f, \quad (7)$$

and the skipping singularity occurs when the deflection angle is equal to  $\pm \pi/2$  (classical trapping). Prior to the onset of classical trapping or chaos this singularity does not occur. As has been shown in Ref. [4], the threshold value of the incident angle where the skipping begins to appear makes both factors of Eq. (6) simultaneously zero. The skipping condition can also be expressed in a very useful way in terms of a relation between  $\theta_i$  and  $b$  by substituting Eq. (4) into Eq. (7) as

$$\tan \theta_i(b) = \pm \frac{1 - [\xi'(b)/a]^2}{2|\xi'(b)/a|}. \quad (8)$$

In Fig. 1 we plot this function for the scattering of He atoms from a hard wall model of the Cu(115) surface obtained previously in Ref. [10]. The concave curve presents a minimum at  $b = b^* = 0.22$ , the inflection point of the surface. At an incident angle of  $68.73^\circ$ , the rainbow singularity begins to bifurcate. The region inside the two branches of the curve gives the region of multiple scattering events, or classical trapping which we have demonstrated to be an example of deterministic chaotic scattering, in Refs. [5–7]. Outside that region we have only single scattering events. This threshold value of  $\theta_i^* = 68.73^\circ$  gives the onset of chaos using a hard corrugated wall. According to Eq. (8) no explicit dependence on  $k_i$  appears. On the contrary, when a soft potential [10] (a similarly corrugated Morse potential of well depth 6.35 meV and range parameter  $1.05 \text{ \AA}^{-1}$ ) is used, this value decreases to  $53.2^\circ$  for  $k_i = 10.98 \text{ \AA}^{-1}$ . Thus, for soft potentials the onset of chaos depends on the incident wave vector.

On the other hand, the TR is usually described as a divergence in the slope of the diffracted beam intensity as a function of the incident polar angle at fixed energy. A classical analytical expression of this slope can be obtained from Eq. (2). Thus each

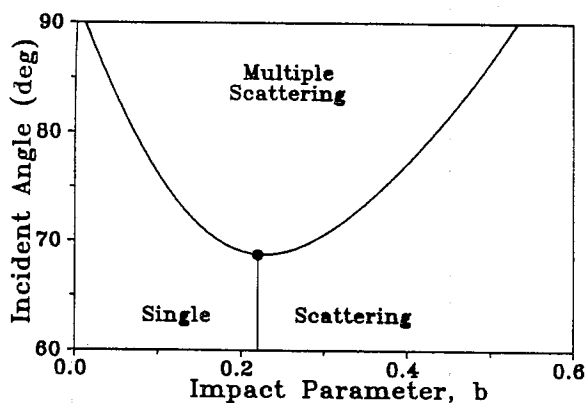


Fig. 1. Bifurcation diagram for the rainbow singularity calculated for the He–Cu(115) system modeled by a hard wall potential. The vertical line represents the location of the rainbow singularity,  $b^* = 0.22$ . At an incident angle of  $\theta_i^* = 68.73^\circ$  the rainbow singularity bifurcates giving rise to two new branches of singularities, the skipping singularities. The region inside the curve corresponds to initial conditions that give rise to chaotic behavior (multiple scattering).

term in the summation in that equation contributes with

$$\frac{dI_J}{d\theta_i} \rightarrow \frac{2\pi}{ak_i} \left( \frac{\sin \theta_f}{\cos^2 \theta_f} \right) \left( \frac{d\theta_f}{db} \right)^{-1}, \tag{9}$$

and therefore the *same singularities* are present in this slope as in the intensity, Eq. (2), from a classical point of view. The only difference now is that here the first factor goes with the square of the cosine function instead of the first power. Three different cases can be envisioned:

- (1) At classical rainbow conditions this slope presents a divergence due to the factor  $(d\theta_f/db)^{-1}$ . However, as shown in Ref. [6], in order for this divergence to be observable in diffraction intensity versus incident angle plots it is necessary that this classical rainbow coincides with an open diffraction channel (quantum rainbow condition). Moreover, this divergence cannot be necessarily associated with a TR condition, since this can occur when there is no emerging beam. To illustrate this point we have carried out close-coupling calculations for the scattering of He atoms from a Cu(115) surface at the quantum rainbow condition for the (30) diffraction peak [6]: incident energy of 63 meV ( $k_i = 10.98 \text{ \AA}^{-1}$ ) and  $\theta_i = 45.9^\circ$ . The corrugated Morse potential has been taken from Ref. [10], and the results for some diffracted peaks versus  $\theta_i$  in the range between  $44^\circ$  and  $47^\circ$ , are shown in Table 1. As can be seen, smooth variations of the diffracted intensities when passing through the value of  $45.9^\circ$  are obtained. The classical rainbow singularity appearing in Eqs. (2) and (9) is not

evident in the quantum mechanical diffraction channel (30) when it fulfills the rainbow condition. This is a clear demonstration that classical singularities are not necessarily reflected in quantum mechanical systems. It is the whole diffraction pattern which has to be associated with a rainbow feature.

- (2) When we are at TR conditions, that is,  $\theta_f = \pm \pi/2$  is a Bragg direction, we have again a divergence in Eq. (9) going as  $\cos^{-2} \theta_f$ . An alternative expression to this equation comes from Refs. [1] and [2] where the origin of TR is in the divergence of the Jacobian derivative of  $k_{Nz}$  with respect to  $\theta_i$ . Thus we have

$$\frac{dI_N}{d\theta_i} = \frac{dI_N}{dk_{Nz}} \frac{dk_{Nz}}{d\theta_i} + \dots, \tag{10}$$

with

$$\frac{dk_{Nz}}{d\theta_i} = (|K_i + N|) \frac{k_{iz}}{k_{Nz}}. \tag{11}$$

Then if  $k_{Nz} = k_i \cos \theta_f = 0$ , or  $\theta_f = \pm \pi/2$ , this derivative also diverges. Note that the factor  $\cos^{-1} \theta_f$  appearing in Eq. (11) is purely kinematical and does not arise from the quantum mechanical solution of the Schrödinger equation. The classical intensity of Eq. (9) varies as  $\cos^{-2} \theta_f$ , and the extra factor  $\cos^{-1} \theta_f$  arises from the explicit evaluation of the classical intensity of Eq. (2). But now the important point is whether the incident angle is less or greater than that corresponding to the onset of chaos,  $\theta_i^* = 53.2^\circ$  at 63 meV for the He–Cu(115) system. In order to illustrate this point we show in Fig. 2 the classical CD function at TR conditions prior to ( $\theta_i = 40.91^\circ$ , Fig. 2a) and after ( $\theta_i = 55.83^\circ$ , Fig. 2b) the onset of chaos, respectively. Horizontal lines show some integer values of the DO function corresponding to some diffracted beams ( $J = 4$  for the (40) diffraction channel, etc.). Prior to the onset of chaos there are no classically allowed trajectories contributing to the emerging (40) diffraction beam. In this case resorting to an analytical continuation of the DO function is necessary [6], and only complex [7] or classically forbidden trajectories (although

Table 1  
Close coupling diffracted intensities for He–Cu(115) scattering at 63 meV

$\theta_i$ ( $^\circ$ )	$I_{00}$	$I_{20}$	$I_{30}$
44.5	0.031	0.146	0.137
45.0	0.039	0.163	0.124
45.5	0.047	0.178	0.111
45.9	0.053	0.189	0.099
46.2	0.059	0.196	0.092
46.5	0.065	0.203	0.086
47.0	0.074	0.214	0.074

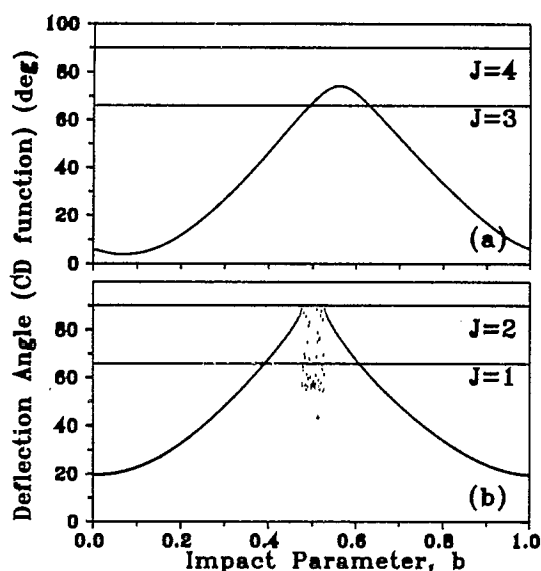


Fig. 2. CD functions for  $E_i = 63$  meV in the scattering of He atoms from the corrugated Morse potential model of the Cu(115) surface: (a) at  $\theta_i = 40.91^\circ$  and (b) at  $\theta_i = 55.83^\circ$ , prior and after the onset of chaos, respectively. Horizontal lines correspond to some integer values of the DO function showing the position of the corresponding diffraction channels.

energetically allowed) contribute to the (40) peak. Furthermore we present in Fig. 3 the variation of some calculated close coupling diffracted intensities ( $I_{00}$ ,  $I_{30}$  and  $I_{40}$ ) versus  $\theta_i$

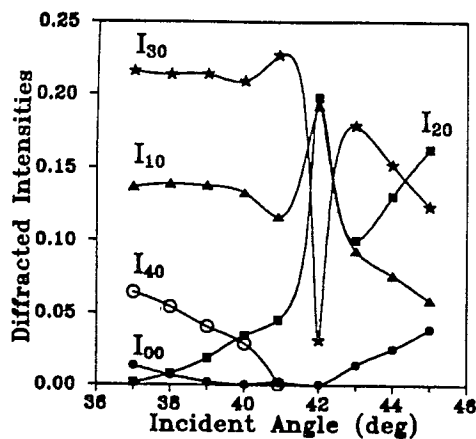


Fig. 3. Close-coupling diffraction intensities for the corrugated Morse potential model of Fig. 2 for He–Cu(115) scattering at 63 meV.

in the range  $37^\circ$ – $45^\circ$  at 63 meV. As can be seen, at  $40.91^\circ$  the peak (40) disappears, leading to strong variations of the rest of the diffracted beams around this incident angle value. *These drastic changes in the curve should be easily observable in scattering experiments.* At this point it is important to remark that at present TRs have not been observed experimentally in atom–surface scattering and these results show that this should not be the case for highly corrugated surfaces.

- (3) When the rainbow begins to bifurcate (minimum of the concave curve in Fig. 1) both factors contribute to the divergence of the slope given by Eq. (9). This case corresponds to the onset of chaos or threshold of classical trapping. In Fig. 2b we show the appearance of the chattering or chaotic scattering region (discrete points) for an incident angle of  $55.83^\circ$  which is greater than  $53.2^\circ$ . At 63 meV this incident angle corresponds to the emergence of the (20) diffraction channel ( $J = 2$  in Fig. 2b). As opposed to the conditions prior to the onset of chaos, only classical chaotic trajectories contribute to the (20) diffracted peak. However, it should be noticed that these trajectories escape from the interaction region with a final scattering angle  $\theta_f = \pi/2$ . They form a special zero measure subset of the chattering region, which never leave the surface since they would reach the asymptotic region only after an infinite time. To give an idea of the topology of these trajectories we present two examples in Fig. 4. The solid line represents a direct classical trajectory belonging to the zero-measure subset of an emerging beam at  $\theta_f = \pi/2$ . Actually it has been calculated at the left border of the chattering region. The dashed line corresponds to a classical trajectory with the same final scattering angle but bouncing twice on the surface. In a similar way trajectories from this subset can be found with any number of bounces on the surface considering the (fractal) chattering region in Fig. 2b at finer and finer scales [5].

Finally, let us point out that only in this third case does the name *resonance* truly apply in a classical context, in the sense that the He atoms

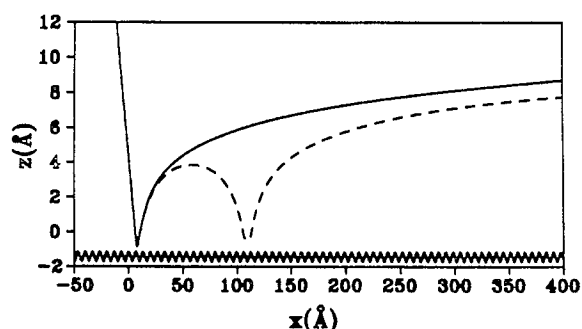


Fig. 4. Two representative trajectories for He–Cu(115) scattering at 63 meV and incident angle of  $55.83^\circ$ . They belong to the zero measure subset of the chattering region shown in Fig. 2b that leave the surface with a final scattering angle of  $\pi/2$ . See text for details.

spend part of their time making multiple collisions with the surface. Another important point is the following: when  $\theta_i$  is above the threshold value  $\theta_i^*$  for chaotic behavior and the chattering region is large, the contributions of a large number of chaotic trajectories become important and cause an enhancement of the intensities at TR conditions. For weakly corrugated surfaces this fact could be exploited as a means to enhance the effect of TR.

### Acknowledgements

This work has been supported in part by DGICYT-Spain (projects no. PB93-0454, PB95-425 and PB95-0071) and by the NSF (grant no.

DMR9419427). R.G. gratefully acknowledges a doctoral grant from the Ministerio de Educación y Ciencia, Spain. S.M.A. and J.R.M. thank the MPI für Strömungsforschung for providing a stimulating environment during part of this work. S.M.A. gratefully acknowledges the Alexander von Humboldt Foundation for a Fellowship.

### References

- [1] N. Cabrera and J. Solana, in: Proc. Intern. School of Physics Enrico Fermi, Ed. F.O. Goodman (Compositori, Bologna, 1974) p. 530;
- N. Garcia, Surf. Sci. 71 (1978) 220;
- N. Garcia and W.A. Schlup, Surf. Sci. 122 (1982) L657.
- [2] G. Armand and J.R. Manson, Surf. Sci. 169 (1986) 216.
- [3] K.B. Whaley, C. Yu, C.S. Hogg, J.C. Light and S.J. Sibener, J. Chem. Phys. 83 (1985) 4235.
- [4] S. Miret-Artés, J. Margalef-Roig, R. Guantes, F. Borondo and C. Jaffé, Phys. Rev. B 54 (1996) 10 397.
- [5] F. Borondo, C. Jaffé and S. Miret-Artés, Surf. Sci. 317 (1994) 211.
- [6] R. Guantes, F. Borondo, C. Jaffé and S. Miret-Artés, Surf. Sci. 338 (1995) L863.
- [7] R. Guantes, F. Borondo, C. Jaffé and S. Miret-Artés, Phys. Rev. B 53 (1996) 14 117.
- [8] R. Guantes, F. Borondo and S. Miret-Artés, to be submitted.
- [9] R.I. Masel, R.P. Merrill and W.H. Miller, J. Chem. Phys. 64 (1976) 45.
- [10] S. Miret-Artés, J.P. Toennies and G. Witte, Phys. Rev. B 54 (1996) 5623.
- [11] W.H. Miller and T.F. George, J. Chem. Phys. 56 (1972) 5668;
- J. Stine and R.A. Marcus, Chem. Phys. Lett. 15 (1972) 536.